Synthesis and characterization of a fluorinated poly(imide–siloxane) copolymer: a study of physical properties and morphology

John J. Fitzgerald*, Scott E. Tunney and Michael R. Landry
Research Laboratories, Eastman Kodak Company, Rochester, New York 14650, USA
(Received 10 April 1992; revised 6 July 1992)

Dynamic mechanical analysis (DMA), small-angle X-ray scattering (SAXS), and transmission electron microscopy (TEM) have been used to characterize the physical properties and morphology of a series of poly(imide–siloxane) copolymers. These copolymers based on DAPI-6F contain either a short bis(aminopropyl) terminated siloxane monomer or oligomer. The results show that the copolymers containing the oligomeric segments are phase separated. The SAXS results indicate that the domain size of the poly(dimethylsiloxane) segment is independent of the siloxane-to-imide ratio. However, the DMA results show that the high temperature maximum in E'', herein defined as T_g of the imide phase, decreases with an increasing amount of the oligomeric siloxane. It is suggested that the depression of T_g may be the result of lowering of the molecular weight of the imide segments.

(Keywords: poly(imide–siloxane) copolymers; SAXS; TEM; DMA)

INTRODUCTION

Polyimides are widely used for high-performance applications because of their high glass transition temperature, excellent thermal and hydrolytic stability, and chemical resistance[1]. For uses in the electronic packaging industry where mechanical stability and electrical properties have critical tolerance limits for acceptable performance, the affinity of many polyimides to absorb moisture is a serious concern. Further, the conventional processing method of using polyimide intermediates that are coated from strongly interacting solvents such as *N*-methylpyrrolidinone (NMP) followed by high temperature cures and long bake times often results in the formation of intractable materials[2,3].

Reducing the propensity for moisture uptake by polyimides has been an active area of study in our laboratories. To this end, fluorinated polyimides have been explored. Additionally, to enhance the solubility characteristics, recent activity has been aimed towards the design and synthesis of polyimides which incorporate flexible units in the backbone[4,5]. One successful example is the polycondensation of poly(dimethylsiloxane) (PDMS) and polyimides. The combination of a siloxane block with an imide has not only been shown to increase the solubility of the polymer, but also to improve its u.v. stability, resistance to ozone, and adhesion to metals[6–8].

Additional incorporation of a non-planar, unsymmetrical, yet rigid monomer into the polyimide backbone is another approach for improving the solubility characteristics. Therefore, the polyimide DAPI-6F has been highlighted in our studies. DAPI-6F is formed from a condensation reaction of 5-amino-(4-aminophenyl)-1,1,3-trimethylindane[9,10], which in shortened notation is diaminophenylindane or DAPI, and 2,2-bis(4-phthalic anhydride)hexafluoroisopropylidene (6F). The DAPI monomer adds an 'unsymmetrical kinked' character to the polyimide backbone, and the 6F molecule adds solubility. Therefore, it was expected that this polyimide would be very soluble. At the same time, this material has low moisture sensitivity and a low dielectric constant.

While these new fluorinated poly(imide–siloxane) copolymers possess important practical aspects, they exhibit novel morphological and mechanical features as well. It is well known that chemical differences within segregated copolymer chains often lead to microphase separation in the bulk state, provided the requirements for thermodynamic incompatibility are met[11]. Characterization by transmission electron microscopy (TEM), small-angle neutron scattering (SANS), dynamic mechanical analysis (DMA), and small-angle X-ray scattering (SAXS) of structural features for a few poly(imide–siloxane) materials of high siloxane content has been reported[12–14]. Curiously, phase separation is seen to exist not only at the microscopic (50–200 Å) scale, but also at scales of 10–100 μm[12,13].

In this report we present the results of a study of the morphology and physical properties of DAPI-6F copolymers containing either a short bis(aminopropyl) terminated siloxane comonomer, α,ω-bis(aminopropyl)-tetramethyl-disiloxane [Si2], or an oligomeric one, Si50. The techniques utilized include DMA, TEM, and SAXS. Extensive emphasis is placed on the latter method in order to describe quantitatively the morphology of these materials. It is hoped that relationships can be established between the physical properties and the morphology.

* To whom correspondence should be addressed

0032-3861/93/091823-10

Table 1 Characterization of DAPI(X)Si(Y)-6F copolymers

Mol% of siloxane oligomer, X $Y=2//X=$	Wt% dimethylsiloxane	IV (dl g^{-1})	Yield (%)
10	2.2	0.40	99
20	4.4	0.41	98
$Y=50//X=$			
0.4	2.2	0.72	99
0.8	4.2	0.75	99
2	9.9	0.72	97
5	21.7	0.87	93
10	36.0	0.53	96
DAPI-6F	0	0.68	99

EXPERIMENTAL

General method for polyimide preparation

The polyimides were prepared at room temperature by the addition of an equal molar amount of the dianhydride to a solution of the diamine(s) in tetrahydrofuran (THF) at 20% solids. The reaction was then stirred under ambient conditions overnight. To this mixture were added 3.5 molar equivalents of pyridine and 4.0 molar equivalents of acetic anhydride, followed by overnight stirring. The dissolved polymer was precipitated into methanol (MeOH), and the resultant fibrous product was chopped in a Waring blender. The polymer was isolated by vacuum filtration, washed with MeOH and dried at 100°C for 12 h under vacuum. Inherent viscosities of all the polymers were determined in *N,N*-dimethylacetamide at 0.5 g dl^{-1}, 25°C and are given in *Table 1*.

A schematic of the synthesis is given in *Figure 1*. For completeness, details of a synthesis for one of the copolymers, DAPI(10)Si2-6F (the nomenclature is described later) are given here. The polyimide was prepared from 9.590 g (0.036 mol) of DAPI, 0.994 g (0.004 mol) of Si2, and 17.770 g (0.040 mol) of 6F in 113 g THF. The polyamic acid was imidized by the addition of pyridine (11.1 g, 0.140 mol) and acetic anhydride (16.3 g, 0.160 mol), and the resulting polyimide was isolated to give 26.64 g (99% yield), IV = 0.40 dl g^{-1}.

The 6F monomer, 2,2-bis(4-phthalic anhydride)hexafluoroisopropylidine, was obtained from Hoechst–Celanese. DAPI, 5-amino-(4-aminophenyl)-1,1,3-trimethylindane, was obtained in-house. Apart from the siloxane materials, all other chemicals were obtained from Eastman Kodak Company. The siloxane dimer Si2, α,ω-bis(aminopropyl)tetramethyl disiloxane, was purchased from Petrarch Chemical. The aminopropyl terminated dimethylsiloxane oligomer Si50 was synthesized by Dr Timothy Long. Its number-average molecular weight, determined by endgroup titration, is 3840 g mol^{-1}, corresponding to an average of approximately 50 dimethylsiloxane units per molecule, hence the acronym Si50. The characteristics of the copolymer samples are summarized in *Table 1*. The copolymers are designated DAPI(X)SiY-6F, where the quantity X indicates the mol% of the bis(aminopropyl) terminated siloxane (by endgroups) relative to the overall diamine content, and the quantity Y indicates the siloxane monomer size ($Y=2$ or 50).

A cross-linked film of PDMS was prepared for examination by SAXS. A divinyl terminated poly(dimethylsiloxane) oligomer (Petrarch Chemical, PS441, $M_n=4860$, $M_w/M_n=2.4$ by GPC-LALLS) was reacted with a stoichiometric amount of a tetrafunctional cross-linker, tetrakis(dimethylsiloxy)silane (Petrarch Chemical, T1915) using Pt[$(C_2H_5)_2S$]$_2Cl_2$ at 20 ppm per chain end as a catalyst. The free-standing film was formed by knife coating the PDMS/cross-linker mixture and allowing it to stand for approximately 1 h in air with slight heating from a laboratory hotplate.

Thermal analysis

A Perkin–Elmer TGS-2 TGA was used to determine the thermal stability of the polymers at a scanning rate of 10°C min^{-1} in an ambient atmosphere. The TGS-2 was attached to a Perkin–Elmer 3600 Data Station. A Mettler Thermomechanical Analyzer (TMA) was used to measure the thermal coefficient of expansion (t.c.e.) of the poly(imide-siloxane) films. The heating rate was 5°C min^{-1}, and the average t.c.e. between −30 and 50°C was calculated.

Dynamic mechanical analysis

A Rheometrics Solids Analyzer II (dynamic mechanical analyser, DMA) was used to measure the viscoelastic response of knife-coated polymer films. The temperature was scanned at 2 to 3°C min^{-1} at a frequency of 10 Hz. The maximum in the loss modulus, E'', was defined as T_g.

Transmission electron microscopy

Two samples with the highest PDMS content in the Si50 series, DAPI(10)Si50-6F and DAPI(5)Si50-6F, were examined by TEM. Ultrathin sections of approximately 70 nm in thickness were sliced normal to the knife-coated film surfaces. The solvent used for the knife coatings was methylene chloride. Prior to sectioning, the samples were embedded in a 2.1 M sucrose solution and sectioned at −60°C. The sections were prepared with a Reichert–Jung Ultracut E microtome with a FC4 cryo-attachment. Micrographs were taken with a JEOL 110CXII transmission electron microscope. Due to the electron density contrast difference between the PDMS and DAPI-6F polyimide phases, no staining was necessary.

SAXS measurements

Small-angle X-ray scattering measurements were performed on knife-coated films of the poly(imide-siloxane) copolymers. Typically four to six film strips, 0.05 mm thick, were stacked and examined normal to their surfaces. A 0.5 mm thick cross-linked strip of PDMS

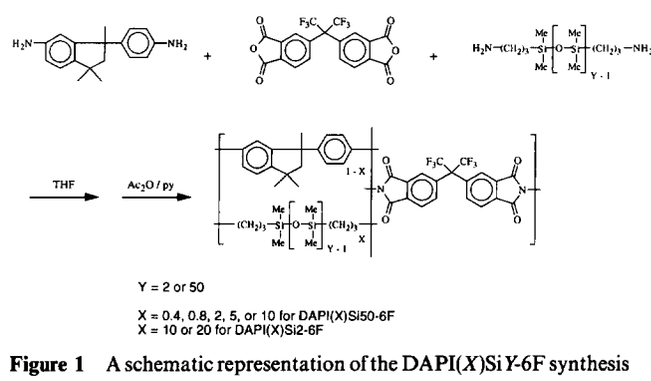

Figure 1 A schematic representation of the DAPI(X)SiY-6F synthesis

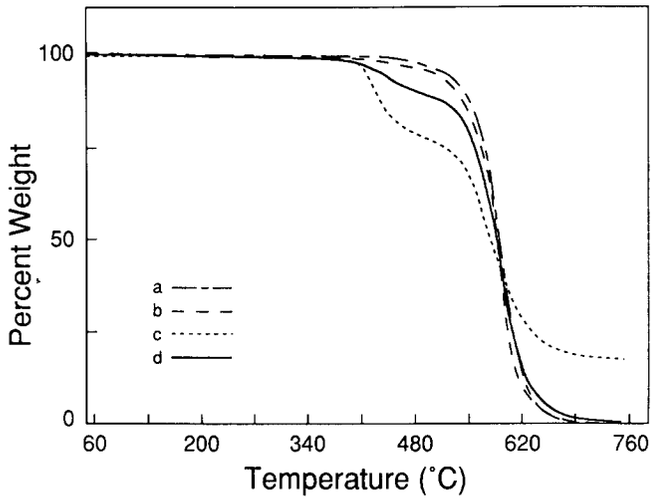

Figure 2 TGA curves for: (a) DAPI-6F; (b) DAPI(0.8)Si50-6F; (c) DAPI(10)Si50-6F, and (d) DAPI(20)Si2-6F

was also examined. All SAXS profiles were recorded with a compact Kratky camera (Anton Paar) equipped with a one-dimensional position sensitive detector (PSD) (M. Braun, model OED-50M). The X-ray source was a Ni filtered beam from a line focus of a sealed Cu anode X-ray tube operated at 35 kV, 15 mA by a Siemens Kristalloflex K710H generator. The CuKα peak of the X-ray source was selected with an energy discriminator. Two sample-to-detector distances (SDD) were employed. For higher resolution at small values of the scattering vector q, SDD = 740.5 mm. A distance of 254.5 mm was used to record the higher angle regions of the SAXS profiles, up to $q = 0.6$ Å^{-1}, where $q = (4\pi/\lambda)\sin(\theta/2)$ and θ, λ are the scattering angle and X-ray wavelength, respectively. The incident beam dimensions defined by the collimation system of the Kratky camera were set to 20 mm by 0.05 mm. All of the scattering curves were corrected for detector inhomogeneity by illumination with an iron-55 source, parasitic scattering, and normalized for sample thickness, transmittance, and incident beam intensity. Intensities were recorded in arbitrary units.

Several SAXS data analysis procedures commonly used to investigate two-phase materials[15] were employed to analyse the scattering profiles for the copolymer films. When applicable, Guinier plot analyses were used to obtain a domain radius of gyration, R_g. Domain spacings d were determined by applying Bragg's law to SAXS curves that exhibited scattering peaks. For Guinier plot and Bragg spacing analysis, desmearing of the slit-smeared SAXS profiles was performed using Glatter's iterative desmearing method[16]. Prior to the desmearing operation, each of the scattering curves was adjusted for a positive upturn in the scattering behaviour at high angles. This upturn is commonly assigned to local electron density fluctuations and/or the onset of wide-angle scattering within the polymer samples. Details about the subtraction of this high angle background are discussed in the Results section. The background-corrected profiles were subsequently smoothed by a funnelling[17,18] or cubic spline procedure. In the funnelling procedure, a variable number of intensity values are averaged according to the counting statistics of the data set.

RESULTS AND DISCUSSION

Synthesis

Polyimides are generally prepared by a two-step process. The first step is the condensation of a diamine with a dianhydride to give a polyamic acid. The polyamic acid is imidized by either chemical or thermal means to give the polyimide. Many of the problems with utilizing polyimides for the fabrication of electronic devices have been associated with lack of solubility of the polyimide in common organic solvents. To circumvent the insolubility issue, classically most polyimides are processed in the polyamic acid form, then thermally cured to give the polyimide. Full conversion usually requires the use of high temperatures and long bake times. These difficulties are not encountered with these new fluorinated polyimides DAPI-6F, DAPI(X)Si2-6F, and DAPI(X)Si50-6F. Each of these materials was fully imidized in solution and is soluble in common organic solvents such as 1,1,1-trichloroethane and methylene chloride.

Thermal stability

The TGA results indicate that the major onset of weight loss for DAPI-6F occurs at 562°C. Similar to the results reported by McGrath and coworkers[3,19], poly(imide–siloxanes) generally have good thermal stability. However, as shown in *Figure 2*, a reduction in the thermal stability of the polymer is observed with increasing siloxane content presumably because of the introduction of the *n*-propyl segment to link the siloxane into the structure. For the copolymer DAPI(10)Si50-6F, the reduction of the thermal stability compared with the homopolymer is of the order of 153°C. In addition, while DAPI(0.8)Si50-6F and DAPI(20)Si2-6F contain approximately equal amounts of dimethylsiloxane, the results shown in *Table 2* indicate that as the molecular weight of the siloxane component is decreased the thermal stability of the polymer is reduced. This is attributed to the greater percentage of the *n*-propyl segments incorporated into the polymer.

Dynamic mechanical properties

The dynamic mechanical properties of the homopolymer of DAPI-6F and each of the siloxane modified polyimides were studied. The storage and loss moduli of DAPI-6F are shown in *Figures 3a* and *3b*, respectively. It should be noted that the transition from glass-to-rubbery-to-terminal region is fairly sharp for this homopolymer.

Table 2 TGA and DMA results

Polymer	Onset of major weight loss (°C)	Glass transition temperature[a] (°C)	
		Siloxane phase	Imide phase
DAPI-6F	562	–	336
DAPI(0.4)Si50-6F	562	−115	320
DAPI(0.8)Si50-6F	562	−117	318
DAPI(2)Si50-6F	553	−121	309
DAPI(5)Si50-6F	414	−133	273
DAPI(10)Si50-6F	409	−133	254
DAPI(10)Si2-6F	564	–	293
DAPI(20)Si2-6F	409	–	261

[a] Glass transition temperature taken from DMA data

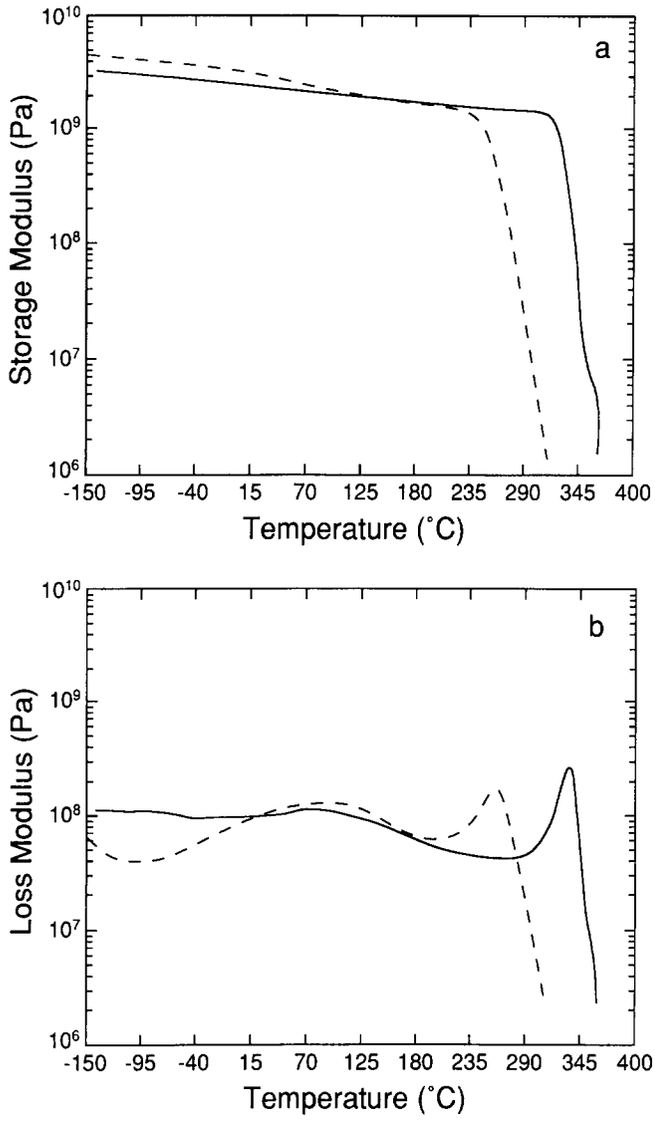

Figure 3 (a) The storage modulus E' as a function of temperature for the polyimide DAPI-6F (solid), and the copolymer DAPI(20)Si2-6F (dashed). (b) The loss modulus E'' for DAPI-6F (solid) and DAPI(20)Si2-6F (dashed)

Moreover, the loss peak centred at 336°C is fairly narrow and well defined. A broad loss peak attributed to secondary relaxations in the polymer is also observed, centred at about 90°C. In *Figures 3a* and *3b* the DMA trace of DAPI(20)Si2-6F is also shown. For this copolymer, a very broad secondary loss peak is observed between −40°C and about 180°C. In addition, the temperature at which the maximum loss peak in E'' occurs is reduced to about 261°C. The reduction in T_g is thought to be due to the introduction of the flexible spacer units (Si2) that are randomly distributed in the backbone of the polymer. No low temperature loss peak, attributable to the relaxation of siloxane phase, is observed.

Figures 4a and *4b* display the dynamic mechanical analysis results for the Si50 modified polyimides. Two distinct primary maxima in the loss peak curves are observed, separated by a broad secondary loss peak. The intensity of the intermediate peak appears to scale with the concentration of the DAPI-6F present. For DAPI(0.4), DAPI(0.8) and DAPI(2), the low temperature loss peak is centred near −120°C, *Table 2*, and is assigned to the T_g of the siloxane phase. As indicated in *Table 2*, both DAPI(5) and DAPI(10) also exhibit a broad low temperature loss peak but, curiously, the maximum is near −133°C. The observation of a loss peak at this low temperature appears to be inconsistent with previously reported values of T_g for a siloxane phase[19,20]. Further dynamic mechanical studies on these samples show that the position of the low temperature peak is reproducible over a two-year period. Moreover, in one experiment, the sample was held at −150°C for 30 min to ensure thermal equilibrium was attained. Once again the position of the low temperature maximum was measured at −133°C. While the glass transition temperature of the siloxane phase measured by DMA is lower than other reported values for siloxane–imide copolymers, it may be the result of the low molecular weight siloxane block that was used. The equilibration reaction used to prepare the aminopropyl terminated siloxane block usually produces a polydispersity of greater than 2. Therefore, a significant amount of low molecular weight fraction would be expected (M_n below 3000 g mol^{-1}). As discussed by Clarson *et al.*[21], the T_g of linear PDMS is strongly dependent on the molecular weight of the polymer below

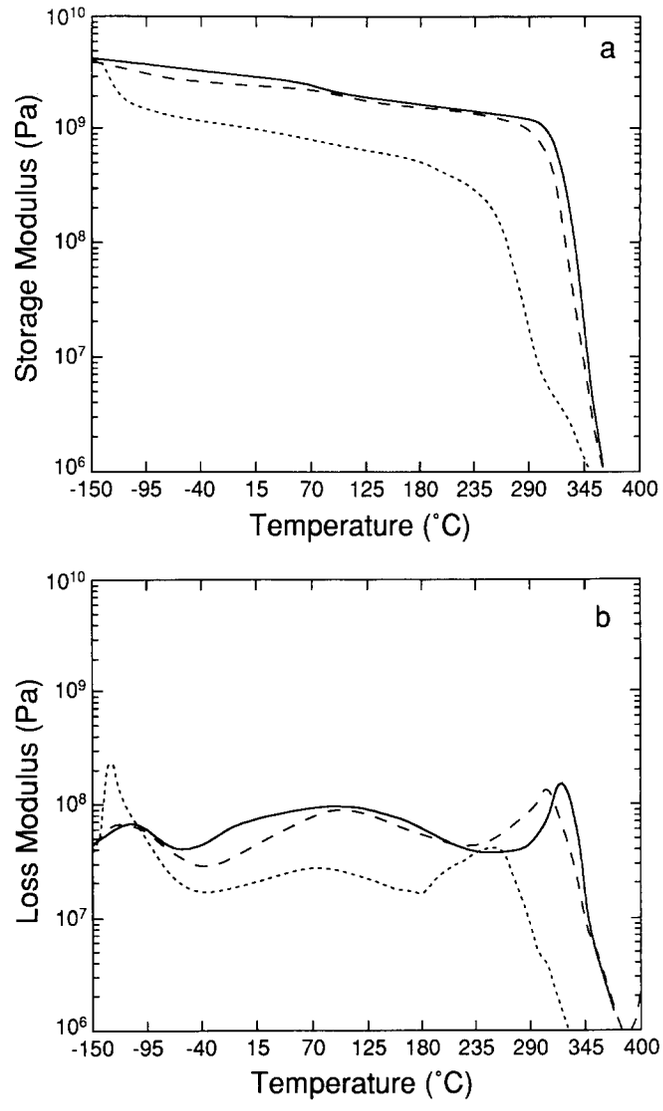

Figure 4 (a) The storage modulus E' for DAPI(0.4)Si50-6F (solid), DAPI(2)Si50-6F (dashed), and DAPI(10)Si50-6F (dotted) and (b) loss modulus E'' for DAPI(0.4)Si50-6F (solid), DAPI(2)Si50-6F (dashed), and DAPI(10)Si50-6F (dotted) as a function of temperature

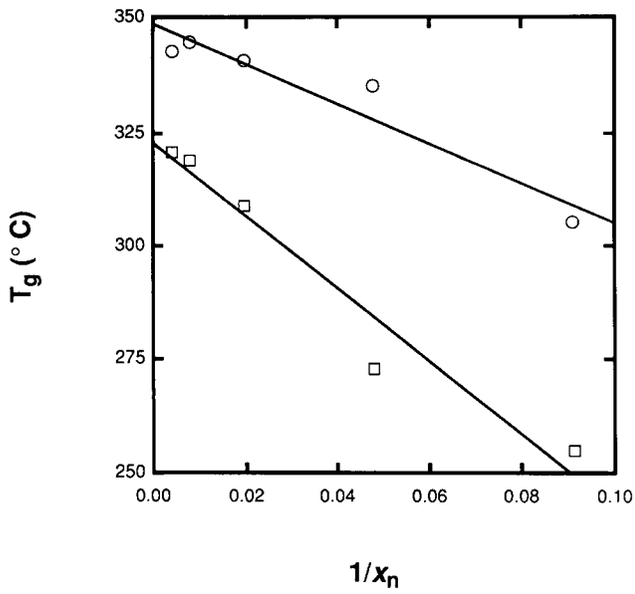

Figure 5 A plot of the polyimide phase glass transition temperature T_g taken from E'' (□) and tan δ (○) as a function of $1/x_n$, the reciprocal of the number average degree of polymerization of the polyimide segments calculated from equation (1)

3000 g mol^{-1}. Therefore, it is not unexpected to observe a T_g of less than −123°C for these copolymers.

The high temperature loss peak (*Figures 4a* and *4b*) is associated with the polyimide phase and is seen to decrease with increasing concentration of the siloxane component. As an example, with the introduction of 10 mol% DAPI(10)Si50-6F, a reduction in the glass transition temperature from 336°C to 254°C is observed. The breadth also increases with the addition of the siloxane block, attaining a width of the order of 60–80°C for the highest siloxane content.

It has been previously reported that for block copolymers containing a glassy and rubbery phase, i.e. styrene and butadiene, the position of the high-temperature peak shifts to lower temperature with increasing concentration of the butadiene segments[22,23]. However, the position of the low-temperature maximum in these reports was unchanged and was similar to that of the polybutadiene homopolymers. Also, the high temperature peak of the styrene–butadiene block copolymers did not show substantial broadening, nor did its width vary with increasing concentration of polybutadiene segments. Based on their results the authors concluded that the shift in T_g of the glassy phase was due to an increase in the amount of phase mixing. A similar observation for poly(imide–siloxane) copolymers containing shorter (M_n=900, or Si12 in our notation) oligomers was reported by Arnold *et al.*[20]. It was suggested that the depression in T_g was due to phase mixing. However, for the imide–siloxane copolymers in this report, the SAXS results which appear later do not indicate any appreciable phase mixing. Rather, we propose that the decreasing imide phase T_g is due to a reduction in the imide block molecular weight, as noted by Kambour for a series of poly(carbonate–siloxane) copolymers[24].

To pursue this last point, we assume that the Si50 siloxane oligomers impart enough mobility to the system that the imide blocks relax independently. One can therefore examine the molecular weight dependence of the polyimide phase T_g, as shown in *Figure 5* plotted as T_g *versus* $1/x_n$, where x_n is the number average degree of polymerization of the polyimide 'blocks' calculated from:

$$\bar{x}_n = (1+r)/(1-r)$$
$$r = N_A/(N_A + 2N_B) \quad (1)$$

where N_A and N_B represent the moles of dianhydride and moles of the siloxane diamine, respectively. The latter is taken to behave essentially as a monofunctional monomer in a condensation-type reaction, for which equation (1) is written[25]. Although it is unlikely that the two diamine reactants have equal reactivity, the equilibration step in the polymerization procedure produces a Gaussian distribution of chain lengths[7], which also describes condensation polymerizations of monomers of equal reactivity. While all of the assumptions used to arrive at the plot in *Figure 5* may not be rigorous, it is felt that the dependence shown supports the idea that the higher glass transition temperature change is due to the variation in the polyimide block molecular weight. The T_g values in *Figure 5* are taken from the E'' *versus* temperature data in *Figure 4b* and tan δ *versus* temperature plots (not shown).

Thermal coefficient of expansion

Samples were run in the tensile mode on the thermal mechanical analyser in order to determine the average thermal coefficient of expansion (t.c.e.) between −30 and 50°C for the pure DAPI-6F and each of the copolymers. As shown in *Figure 6* a nearly linear increase in t.c.e. is observed with increasing concentration of the randomly incorporated Si2 segments and of the block siloxanes (Si50). It is interesting to note that at similar wt% loadings of the dimethylsiloxane, the t.c.e. values of the Si2 and Si50 are similar. The linear increase of t.c.e. for the oligomeric Si50 series is difficult to understand. To our knowledge, there is no applicable theory to predict how the t.c.e. should vary with block length or concentration in a block copolymer. The linear mixing rule was successfully applied by Diament and Williams[26] to describe the linear increase in t.c.e. for styrene–butadiene–

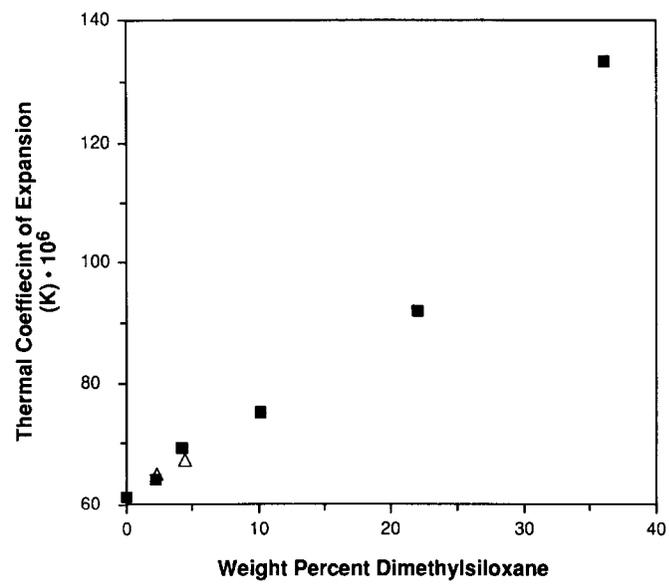

Figure 6 The thermal coefficient of expansion (t.c.e.) plotted against the wt% Si for the poly(imide–siloxane) copolymers. *Table 1* shows the wt% of the copolymers

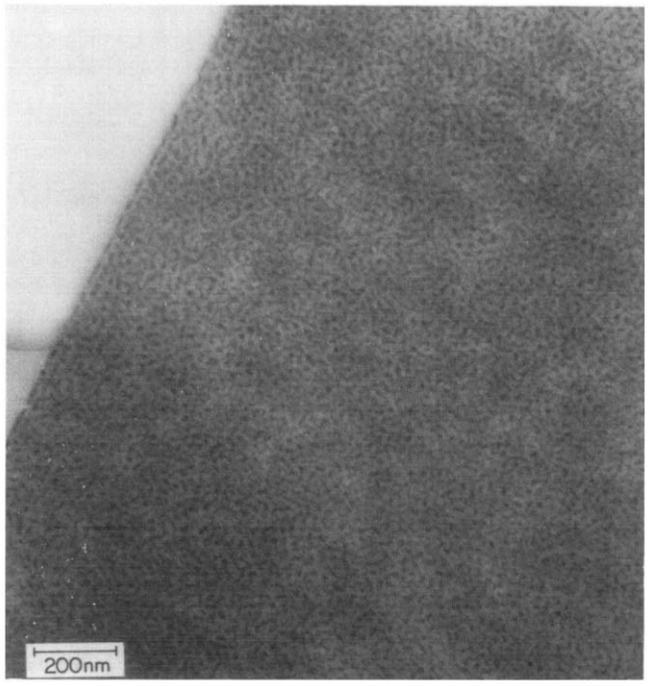

Figure 7 A TEM cross-section of unstained DAPI(5)Si50-6F. Note the surface segregation of the darker PDMS phase and the distinct two-phase morphology in the bulk of the sample

styrene copolymers. However, the linear mixing rule is designed to apply to isotropic systems with perfect adhesion at the phase interface. Moreover, it has been applied mostly to account for changes in the thermal coefficient of expansion of systems filled with rigid particles in an amorphous matrix.

Morphology: TEM results

A TEM image of a sectioned DAPI(5)Si50-6F copolymer film is shown in *Figure 7*. A distinct two-phase morphology is present, with the darker microphase being attributed to the PDMS domains. Note that one of the free film surfaces is included in the micrograph where an excess of the PDMS is apparent. No elemental analysis of the surface was performed to confirm this observation, although there is evidence in the literature of surface segregation of PDMS for another poly(siloxane–imide) multiblock copolymer[3]. Similar images were observed for the DAPI(10)Si50-6F material but are not shown here. A biphasic microstructure similar to the one shown in *Figure 7* has been observed by Spontak *et al.*[12] and York and coworkers[27] for other poly(siloxane–imide) copolymers. Qualitatively, it is observed for the DAPI(5)Si50-6F copolymer that the siloxane-rich microdomains are reasonably uniform in size and are separated uniformly by the polyimide phase. Remarks as to quantifying the domain size and spacings for the Si50 series of copolymers are presented with the SAXS results which follow. No microscopy was done on the Si2 series.

Morphology: SAXS results

The microphase separated Si50 materials were analysed in detail by small-angle X-ray scattering. To appreciate fully and understand the various parameters used to describe quantitatively the morphology of these samples, aspects of the analysis procedure are reviewed when necessary.

First, the interfacial nature of the phase separated samples is analysed. To probe the interface of the biphasic structures observed by TEM, we first focus on the intermediate and high angle portions of the scattering profiles (represented as intensity I *versus* scattering vector q), that is, where $R_g > q^{-1} \gg a$. R_g and a represent the radius of gyration of a heterogeneity and a covalent bond or monomer length in the backbone, respectively. Porod[28] has shown that for multiphase structures with sharp phase boundaries (i.e. 'infinitely narrow' interfaces), the scattering intensity $I(q)$ falls off as:

$$\lim_{q \to \infty} I(q) = K_p / q^{\alpha} \qquad (2)$$

where K_p is related to the surface-to-volume ratio in the heterogeneous material, and the exponent α equals 4.0 for pinhole collimation. For slit smeared scattering curves, as are obtained with the Kratky optics used in this study, $\tilde{I}(q) \propto q^{-3}$, where the tilde ($\sim$) denotes the smeared intensity. A diffuse interface leads to negative deviations from ideal Porod power law behaviour[29]. Opposing this effect is a contribution due to density fluctuations and liquid-like scattering within the phases, which is manifested by an increased background, hence an exponent $\alpha < 3$ for slit smeared scattering profiles (cf. equation (2)).

Prior to the actual background correction, we sought to examine the high angle regions of the scattering profiles which were recorded with the shorter of the two sample-to-detector distances. *Figure 8* displays the baseline (high angle) portion of the SAXS curves for each of the Si50 poly(imide–siloxane) samples, from 10 mol% to 0.4 mol% PDMS compositions. Included are data for pure DAPI-6F and a cross-linked PDMS specimen. The latter sample was cross-linked in order to generate a free-standing film. It is believed that the presence of the cross-links does not affect the scattering in the Porod region. The profiles in *Figure 8* have been arbitrarily shifted along the ordinate for clarity. Note that for the pure polyimide and the three lowest Si50 materials, a broad feature is visible in the baseline that is not as defined for the two samples with the highest PDMS (5 and 10 mol%) contents; it is completely absent with the PDMS blank. For the 5 and 10 mol% samples, the

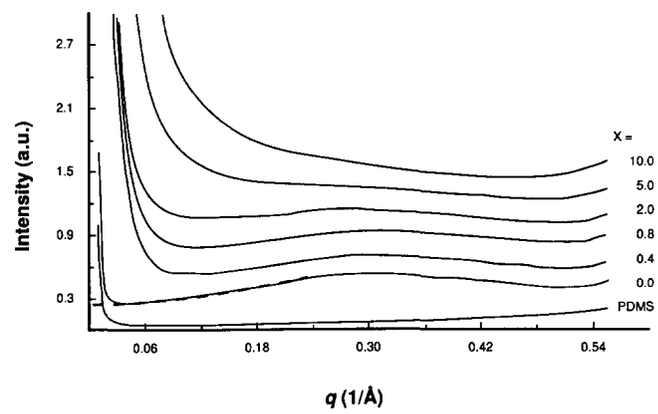

Figure 8 The magnified baseline region of SAXS profiles for a PDMS blank (bottom), the pure polyimide DAPI-6F (2nd from bottom), and the copolymer series DAPI(X)Si50-6F, where $X = 0.4$, 0.8, 2, 5 and 10, in ascending order. The curves have been shifted vertically for clarity, and the low angle features are off-scale. The dashed curve added to the DAPI-6F baseline is an extrapolation according to equation (3)

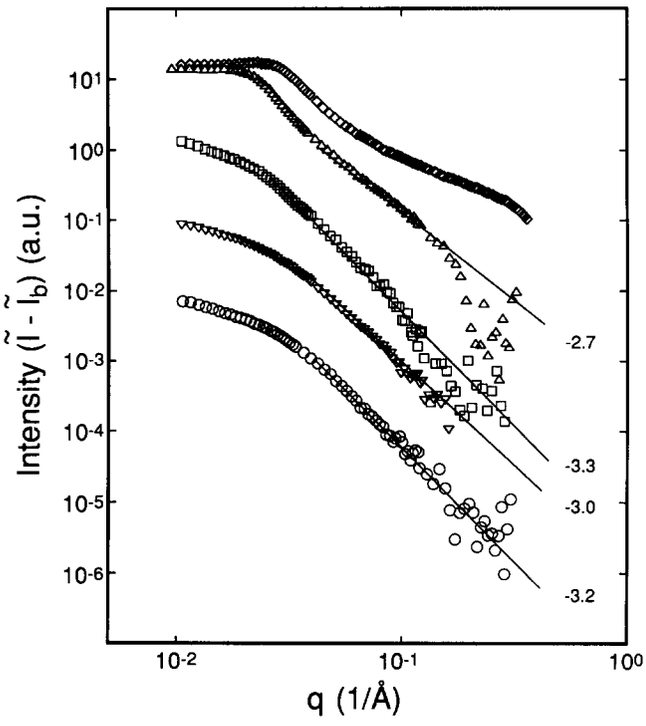

Figure 9 A log–log plot of the baseline-corrected, slit-smeared SAXS intensity ($\tilde{I}-\tilde{I}_b$) *versus* q for the copolymers DAPI(X)Si50-6F, with $X=0.4$ (○), 0.8 (▽), 2 (□), 5 (△) and 10 (◇). The limiting power law slopes are indicated. The profiles have been shifted for clarity

intensity in the baseline region appears to decrease monotonically over the entire scattering vector range because of the enhanced scattering at lower angles. Conversely, the baseline for the pure PDMS film exhibits a gradual increase over the entire region. The broad transition for the polyimide rich samples is attributed to weak liquid-like order in the polyimide phase. As the PDMS content is increased, the contribution to the background scattering of the DAPI-6F phase becomes less dominant as expected, yet the baseline profile does not appear to take on any character of the rubbery PDMS phase as compared with the cross-linked PDMS film blank. This gradual change of the SAXS profiles in the Porod region introduces a complication when trying to correct consistently for the background contribution across the composition series.

There are empirical methods to account for the positive deviations in the background to obtain phase boundary thicknesses, but these methods, by and large, are applied to baselines that show no angular dependence[15,30] or that monotonically increase[31,32]. Rather than using empirical background subtraction methods, the total background was estimated by summing the contributions from the corresponding homopolymers according to volume fraction. This method has been successfully used to account for the background scattering in microphase separated diblock copolymer films[33]. For each subtraction step, the increasing portion of the appropriately weighted baseline on the low q-vector side of the broad transition was fit with the polynomial[31,33]:

$$\tilde{I}_b = aq^n + b \qquad (3)$$

and extrapolated back towards $q=0$. This extrapolation does not influence the Porod law analysis. The dashed line in *Figure 8* added to the baseline for the DAPI-6F homopolymer has been extrapolated to $q=0$ in this manner.

The Porod region of the background corrected, smoothed, and slit smeared SAXS profiles is shown in *Figure 9* in the form of a power law plot, i.e. $\log(\tilde{I}-\tilde{I}_b)$ *versus* $\log q$. For the sake of legibility, the curves have been displaced vertically. Each of the three copolymers with the least amounts of PDMS, i.e. DAPI(0.4), DAPI(0.8) and DAPI(2)Si50-6F, has a limiting slope that is -3.0 or slightly steeper. For the DAPI(5) copolymer, the limiting slope is shallower than -3, and for DAPI(10), no distinct power law is observed. It is possible that for these two samples, the higher volume fractions of the PDMS phases are not properly accounted for by the background subtraction method described above, or that even a very broad and weak second-order Bragg peak is present. (The first-order peaks for DAPI(5) and DAPI(10) are presented below.) Significantly longer data acquisition times and perhaps alternative methods of background subtraction should be attempted to improve analysis of the Porod regions of the profiles shown in *Figure 9*; such experiments are beyond the scope of this study. However, the -3 power law behaviour for the three remaining samples is an indication that smooth (non-fractal) interfaces are present.

A slight negative deviation from ideal Porod law behaviour (i.e. $\alpha \geqslant 3$) is indicative of interfacial mixing between the polyimide and poly(dimethyl siloxane) phases. For the three copolymers exhibiting the approximate Porod law exponent for a smooth interface, the interfacial thicknesses were estimated by the empirical method of Koberstein *et al.*[34] assuming a sigmoidal segment density profile and smearing with an infinite slit. These plots are shown in *Figure 10*. No similar analysis was applied to the SAXS curves for the copolymer samples DAPI(5) and DAPI(10)Si50-6F. Because of the scatter due to low count rates in the Porod region of the SAXS data, the quoted interfacial thickness values listed

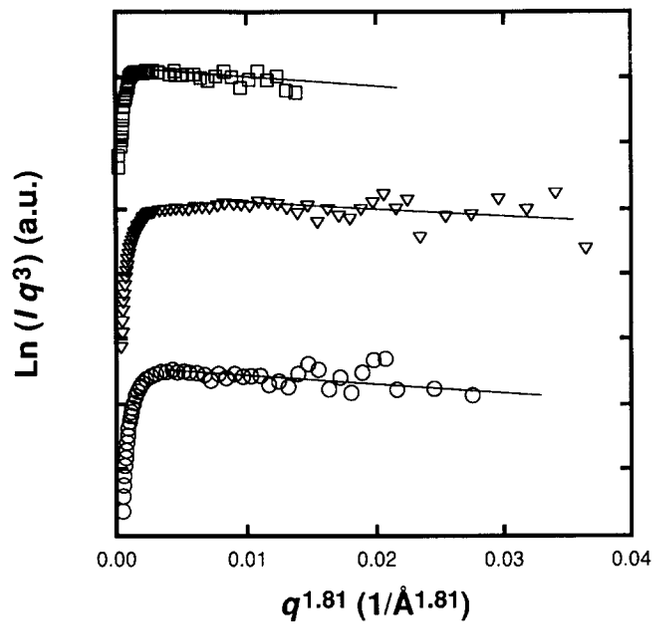

Figure 10 A representation of the empirical method of Koberstein *et al.*[34] for determining interfacial thickness. Only the three samples with the lowest siloxane contents could be analysed. The thicknesses are summarized in *Table 3*. The symbols are the same as in *Figure 9*, and the curves are offset vertically for easier visualization

Table 3 SAXS results for DAPI(X)Si50-6F copolymers

DAPI(X)Si50-6F copolymer $X=$	Porod law exponent α	Interface thickness t(Å)±15–20%	Bragg spacing d(Å)	Radius of gyration R_g(Å)	Teubner–Strey model	
					d(Å)	ξ(Å)
10			232±6		230±5	140±5
5	2.7±0.1		328±6		310±5	150±5
2	3.3±0.1	19.5		83.5±0.5		
0.8	3.0±0.1	16		82.9±0.5		
0.4	3.2±0.05	18		83.7±0.5		

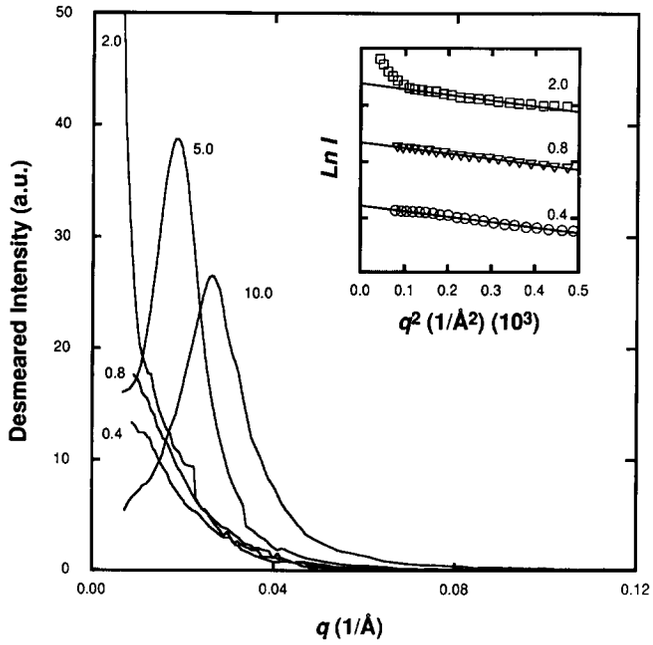

Figure 11 Desmeared SAXS profiles for the five DAPI(X)Si50-6F copolymers, with the values of the siloxane oligomer mole fraction X also provided. The inset shows the Guinier plot used to determine the dispersed domain sizes for three of the samples. The R_g values are summarized in *Table 3*

in *Table 3* are accurate to within only about 15–20%[35], and fall within the range of 16 to 19.5 Å. Nevertheless, these thicknesses give a reasonable indication of the breadth of the interface.

It was noted earlier in the discussion of the polyimide phase glass transition temperature that phase mixing may not be the leading cause of its decrease with increasing Si50 content. For the DAPI(X)Si50-6F materials, the interface thickness values do not indicate appreciable mixing. As a comparative example, conventional diblock copolymers of immiscible components, for example poly(styrene-*b*-isoprene), have interfacial thicknesses between 15 and 20 Å, similar to the values determined in this study, yet exhibit glass temperatures equal to the homopolymer components[36]. However, we cannot rule out the possibility of the imide–siloxane interface being broader for the two samples with the highest Si50 contents, particularly in light of the fact that the number of average degrees of polymerization for DAPI-6F segments are 21 and 11 for $X=5$ and 10, respectively, as calculated from equation (1). One could anticipate some mixing for such short polyimide block lengths, although the results mentioned above are inconclusive. Nevertheless, the observed trend of T_g with $1/x_n$ is still roughly followed for the three samples where the interface width was measured, lending support to the original hypothesis.

Displayed in *Figure 11* are the desmeared SAXS profiles for each of the five copolymers. The two samples with the highest PDMS content show Bragg peaks which infer domain periodicity within the samples. A decrease of the Bragg spacing with increasing PDMS content is expected, since the volume fraction of the polyimide phase is reduced. The remaining three samples produce monotonically decreasing scattering curves which, when fit using a Guinier plot (see inset in *Figure 11*), provide a radius of gyration of 83 Å for the dispersed PDMS phase, although for the copolymer DAPI(2), somewhat larger dispersed particles are also present, indicated by the upturn at low q. These results are also summarized in *Table 3*. The constancy of the dispersed phase size is an interesting observation, in that its value is much larger than expected for the radius of gyration of an unperturbed PDMS chain with a molecular weight of 4000 g mol^{-1}, ca. 15 Å (see ref. 37). This value was calculated for a PDMS chain of 5000 daltons from the experimentally measured R_g of 114.4 Å for a molecular weight of 250 000 g mol^{-1}, with $R_g \sim M^{1/2}$. While a low molecular weight polymer chain, in all likelihood, does not follow Gaussian statistics, this calculation is sufficient for our discussion. With the domains containing several PDMS oligomers, it is unclear as to why these 'clusters' should have similar sizes as the level of PDMS in the copolymer is varied. It is also noted that although the scattering maximum has a lower peak intensity for DAPI(10) when compared with DAPI(5), invariant analysis of all five scattering curves reveals that the total intensity qualitatively tracks with the volume fractions of each phase in the copolymers as expected[15]. For slit smeared intensity $\tilde{I}$, the SAXS invariant Q is defined as

$$Q=\int_0^\infty q\tilde{I}(q)\,dq=2\pi^2V(\rho_1-\rho_2)^2\varphi_1\varphi_2$$

where ρ_i, φ_i are the electron density and volume fraction, respectively, of phase i in the two-phase material of total scattering volume V. Assuming that $(\rho_1-\rho_2)$ remains constant, the invariant is proportional to the product of the volume fractions, which increases throughout the series. The calculated invariant qualitatively follows the same trend.

As a final analysis of the SAXS profiles exhibiting scattering maxima, the model of Teubner and Strey[38] (TS) was examined. This model was originally proposed to explain the origin of a similar SAXS peak from structured microemulsions, and has been recently addressed to analyse the structures in microphase

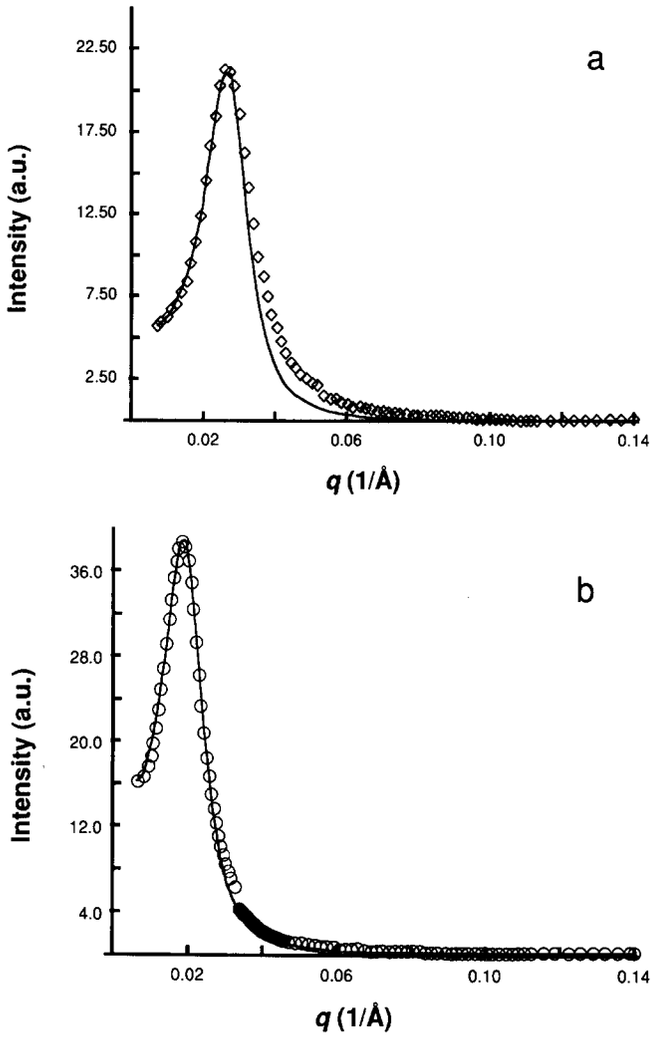

Figure 12 Comparison of the Teubner–Stey model fit (solid line) for desmeared SAXS profiles for (a) DAPI(10)Si50-6F; and (b) DAPI(5)Si50-6F. While the general shape of the scattering maxima is reproduced, the tail region is underestimated because of the sharp interface approximation employed in the model. Results from the fits are summarized in *Table 3*

separated Siltem® poly(imide–siloxane) copolymers[12]. Two length scales d and ξ, representing a domain periodicity and correlation length, respectively, are contained in the expression describing the scattering intensity[39]:

$$I(q) \propto \{[\xi^{-2} + (2\pi/d)^2]^2 + 2[\xi^{-2} - (2\pi/d)^2]q^2 + q^4\}^{-1} \quad (4)$$

In applying the TS model to the desmeared SAXS curves, an arbitrary scaling factor was employed to match the peak heights, while the length scale parameters were varied to obtain fits that best reproduced the profiles near the maxima. The results are shown for copolymers DAPI(5) and DAPI(10)Si50-6F in *Figure 12* and summarized in *Table 3*. While the TS model is able to reproduce the experimental data at scattering vectors before the peak, and also, in general, the peak width, it fails at the higher angles. Inspection of equation (4) shows that an asymptotic q^{-4} dependence is predicted (or q^{-3} for slit smeared data). Experimentally it has already been shown that ideal Porod law behaviour is not observed for these two samples, cf. *Figure 9*, as the limiting power law slope is somewhat shallower than is assumed by the model. Most of the effect of varying the correlation length parameter ξ is in the shape of the profiles near the SAXS maxima, while d affects the peak position along the abscissa. Neither parameter influences the fit quality to any extent in the Porod region. It is concluded that the parameters listed in *Table 3* reasonably quantify the morphology of these samples as described by the Teubner–Strey model. While the domain periodicity varies with PDMS content, the correlation length maintains an approximate value of 150 Å for both samples, roughly twice the R_g measured for the other samples. It is not unreasonable to associate ξ with the size of dispersed siloxane phase, given that its value is approximately constant for the other compositions as well.

CONCLUSIONS

A series of siloxane-fluorinated polyimide copolymers that are soluble in common organic solvents have been designed and synthesized. It has been shown that the thermal stability of these polymers is influenced by the level of siloxane incorporated in the polyimide. For example, thermal gravimetric analysis has shown that incorporation of 10 mol% of the siloxane oligomer into the backbone results in a reduction in thermal stability of 153°C. It is believed that the degradation is initiated by the decomposition of the *n*-propyl linkages.

Dynamic mechanical analysis indicates that the poly(imide–siloxane) copolymers containing the shorter Si2 species are single-phased, a result supported by the SAXS data. In essence, a random copolymer is formed with a glass transition temperature intermediate to that of the pure homopolymer components. These results are in contrast to the DAPI(X)Si50-6F materials which, according to DMA, SAXS and TEM, are distinctly biphasic. In the latter copolymer series, a low temperature transition for the PDMS component and a higher temperature one, which monotonically decreases with increasing mol% Si50, are observed. The reduction in the glassy phase T_g is often interpreted in the literature as being due to phase mixing. However, the analysis of SAXS data indicates that the amount of phase mixing, as noted by the interfacial width, appears unchanged. Instead it is suggested that the reduction of the glass transition temperature may result from the lowering of the molecular weight of the polyimide segments. The attachment of siloxane segments to the ends of the polyimide blocks imparts enough mobility to the system and, in essence, increases the free volume.

ACKNOWLEDGEMENTS

The authors wish to acknowledge the assistance of T. Binga for obtaining the DMA results, P. Hoderlein for the TGA results, and R. Gutierrez for the TEM results. We also wish to thank Dr Timothy Long for the synthesis of the PDMS oligomer and Dr James O'Reilly for valuable discussions.

REFERENCES

1 Mittle, L. (Ed.) 'Polyimides', Plenum Press, New York, 1984, Vols 1 and 2
2 John, T. V. and Valenty, V. B. In 'Polyimides: Materials,

Chemistry and Characterization' (Eds. C. Feger, M. M. Khojastch and J. E. McGrath), Elsevier, Amsterdam, 1989, p. 91
3 Arnold, C. A., Summers, J. D., Chen, Y. P., Bott, R. H., Chen, D. and McGrath, J. E. *Polymer* 1989, **30**, 986
4 Burks, H. D. and St. Clair, T. L. In 'Polyimides: Synthesis, Characterization, and Applications' (Ed. K. L. Mittal), Plenum Press, New York, 1984, Vol. 1, pp. 117–135
5 Critchley, J. P. and White, M. A. *J. Polym. Sci., Polym. Chem. Edn.* 1972, **10**, 1809
6 Yilgor, I., Yilgor, E. and Spinu, M. *ACS Polym. Prepr. Am. Chem. Soc. Div. Polym. Chem.* 1987, **27**(1), 84
7 Yilgor, I. and McGrath, J. E. *Adv. Polym. Sci.* 1988, **86**, 1
8 McGrath, J. E. *J. Adhes.* 1987, **23**, 67
9 Bateman, J. H., Geresy, W., Jr. and Neiditch, D. S. *Proc. of ACS Div — Org. Coat. Plast. Chem.* 1975, **35**(2), 77
10 Faleigno, P., Masola, M., Williams, D. and Jasne, S. 'Polyimides: Materials, Chemistry and Characterization' (Eds. C. Feger, M. M. Khojastch and J. E. McGrath), Elsevier, Amsterdam, 1989, p. 497
11 Helfand, E. and Wasserman, Z. R. In 'Developments in Block Copolymers — 1' (Ed. I. Goodman), Applied Science, London, 1982, pp. 99–125
12 Spontak, R. J., Samseth, J. and Bedford, S. E. *Eur. Polym. J.* 1991, **27**, 109
13 Spontak, R. J. and Williams, M. C. *J. Appl. Polym. Sci.* 1989, **38**, 1607
14 Saraf, R. F., Feger, C. and Cohen, Y. C. In 'Abstracts of the Fourth International Conference on Polyimides', Ellenville, New York, 1991, Session II, p. 45
15 Glatter, O. and Kratky, O. 'Small-Angle X-ray Scattering', Academic Press, New York, 1982, Ch. 2 and 13
16 Glatter, O. *J. Appl. Crystallogr.* 1974, **7**, 147
17 Adapted from Fortran program PDH-(1985) for SAXS data analysis, Anton Paar K. G., A-8054, Graz, Austria, Order No. 17100.06 RSX
18 Fiedel, H. W., Scholler, T., Petermann, J. and Wenig, W. *Colloid Polym. Sci.* 1986, **264**, 1017
19 Arnold, C. A., Summers, J. D., Chen, Y. P., Bott, R. H., Chen, D. and McGrath, J. E. *SAMPE Symp.* 1990, No. 35, 579
20 Arnold, C. A., Summers, J. D. and McGrath, J. E. *Polym. Eng. Sci.* 1989, **29**, 1413
21 Clarson, S. J., Dodgson, K. and Semlyen, J. A. *Polymer* 1985, **26**, 930
22 Bares, J. *Macromolecules* 1975, **8**, 244
23 Kraus, G. and Rollmann, K. W. *J. Polym. Sci., Polym. Phys. Edn.* 1976, **14**, 1133
24 Kambour, R. P. *J. Polym. Sci., Polym. Lett. Edn.* 1969, **7**, 573
25 Flory, P. J., 'Principles of Polymer Chemistry', Cornell University Press, Ithaca, NY, 1953, Ch. 3
26 Diament, J. and Williams, M. C. *Polym. Eng. Sci.* 1986, **26**, 525
27 York, G. A., Waldbauer, R. O., Arnold, C. A., Rogers, M. E., Gungor, A., Rodrigues, D., Wilkes, G. L. and McGrath, J. E. *SAMPE Symp.*, No. 35, 1990, p. 579
28 Porod, G. *Kolloid Z.* 1951, **124**, 83; 1952, **125**, 51; 1952, **125**, 108
29 Ruland, W. *J. Appl. Crystallogr.* 1971, **4**, 70
30 Bonart, R. and Müller, G. H. *J. Macromol. Sci. Phys.* 1974, **B10**, 177
31 Vonk, C. G. *J. Appl. Crystallogr.* 1973, **6**, 81
32 Ruland, W. *Colloid Polym. Sci.* 1977, **255**, 417
33 Hashimoto, H., Fujimura, M., Hashimoto, T. and Kawai, H. *Macromolecules* 1981, **14**, 844
34 Koberstein, J. T., Mora, B. and Stein, R. S. *J. Appl. Crystallogr.* 1980, **13**, 34
35 Roe, R.-J. *J. Appl. Crystallogr.* 1982, **15**, 182
36 Hashimoto, T., Fujimura, M. and Kawai, H. *Macromolecules* 1980, **13**, 1660
37 Kirste, R. G. and Lehnen, B. R., *Makromol. Chem.* 1976, **177**, 1137
38 Teubner, M. and Strey, R. *J. Chem. Phys.* 1987, **87**, 3195
39 Samseth, J., Chen, S.-H., Litster, J. D. and Huang, J. S., *J. Appl. Crystallogr.* 1988, **21**, 835